

# Thermogravimetric analysis-mass spectrometry (TGA-MS) of hydrotalcites containing $\text{CO}_3^{2-}$ , $\text{NO}_3^-$ , $\text{Cl}^-$ , $\text{SO}_4^{2-}$ or $\text{ClO}_4^-$

J. Theo Klopprogge<sup>a</sup>, János Kristóf<sup>b</sup> and Ray L. Frost<sup>a</sup>

<sup>a</sup> Centre for Instrumental and Developmental Chemistry, Queensland University of Technology, 2 George Street, GPO Box 2434, Brisbane, Qld 4001, Australia.

<sup>b</sup> Department of Analytical Chemistry, University of Veszprém, H8201 Veszprém, P.O. Box 158, Hungary.

In 2001. A Clay Odyssey. Proceedings of the 12th International Clay Conference Bahai-Blanca, Argentina, July 22-28, 2001, Dominguez, E., Mas, G. and Cravero, F. (editors), ISBN 0-444-50945-3.

Mg/Al-hydrotalcites containing  $\text{NO}_3^-$ ,  $\text{Cl}^-$ ,  $\text{SO}_4^{2-}$  or  $\text{ClO}_4^-$  were synthesised under  $\text{N}_2$  to prevent incorporation of  $\text{CO}_3^{2-}$ . The presence of the anions in the hydrotalcite structure was confirmed by infrared and Raman spectroscopy. The  $\text{CO}_3$ - and the  $\text{NO}_3$ -hydrotalcites contained both  $\text{NO}_3^-$  and  $\text{CO}_3^{2-}$ , while the Cl-hydrotalcite also contained some  $\text{CO}_3^{2-}$ . It is known that during thermal treatment of hydrotalcites dehydroxylation and decarbonisation strongly overlap. Mass spectrometry following TGA enables one to identify both reactions. For  $\text{CO}_3$ -hydrotalcite  $\text{CO}_2$  is released simultaneously with water (dehydroxylation) around  $335^\circ\text{C}$  followed by NO around  $365$  and  $500^\circ\text{C}$ . The stability of the  $\text{NO}_3$ -hydrotalcite is different showing a major loss of  $\text{CO}_2$  and  $\text{H}_2\text{O}$  (dehydroxylation) around  $410^\circ\text{C}$  with losses of NO around  $345$  and  $450^\circ\text{C}$ . The Cl-hydrotalcite shows a similar behaviour for the  $\text{H}_2\text{O}$  loss (dehydroxylation), but Cl is lost over a range from  $400$  to  $900^\circ\text{C}$  and  $\text{CO}_2$  comes off in steps around  $360$  and  $500^\circ\text{C}$ . Completely different is the thermal behaviour of  $\text{SO}_4$ - and  $\text{ClO}_4$ -hydrotalcites.  $\text{SO}_4$ -hydrotalcite shows a gradual weight-loss due to dehydroxylation with two minor water peaks around  $260$  and  $375^\circ\text{C}$ , while the sulphate remains in the structure. The sulphate is not lost until heated to  $900^\circ\text{C}$ . The  $\text{ClO}_4$ -hydrotalcite shows a complex thermal behaviour with 2 steps of water loss around  $375$  and  $440^\circ\text{C}$ , where the second step is accompanied by the loss of  $\text{O}_2$ . A possible explanation is a redox reaction between perchlorate and the cations giving metal-chlorides and  $\text{O}_2$ .

## 1. INTRODUCTION

Layered double hydroxides (LDHs) are also known as hydrotalcites or anionic clays, due to their layered structure with a charge opposite to that of smectites. The structure of hydrotalcite can be visualised as positively charged OH-layers comparable to those in brucite ( $\text{Mg}(\text{OH})_2$ ) in which a part of the  $\text{Mg}^{2+}$  is substituted by a trivalent metal such as  $\text{Al}^{3+}$  separated by charge compensating, mostly hydrated, anions between the hydroxide sheets. In layered double hydroxides a large range of compositions is possible based on a general formula of  $[\text{M}^{2+}_{1-x}\text{M}^{3+}_x(\text{OH})_2][\text{A}^{n-}]_{x/n} \cdot y\text{H}_2\text{O}$ , where  $\text{M}^{2+}$  and  $\text{M}^{3+}$  are the di- and trivalent metals in the octahedral sites within the OH-sheets with  $x$  normally between  $0.17$  and  $0.33$ .

The number of anions or anionic complexes in layered double hydroxides is essentially unlimited provided that the anion does not form a complex with the cations in the hydroxide sheets during the formation (Vaccari 1998). Therefore, the variety possible in both the cationic and anionic compositions of the hydrotalcite offers the possibility to prepare tailor-made materials for specific applications, such as basic catalysts, as a precursor for the preparation of mixed metal oxidic catalysts, absorbents, as for other specific powder properties such as filler, UV-radiation stabiliser, chloride scavenger and thermal stabiliser (Titulaer 1993).

In some recent publications (Kloprogge et al., 2000, 2002) we have described the incorporation of  $\text{CO}_3^{2-}$ ,  $\text{NO}_3^-$ ,  $\text{SO}_4^{2-}$  and  $\text{ClO}_4^-$  in hydrotalcites and the effects that the confinement of these anions in the interlayer space of hydrotalcites has on their vibrational spectra (infrared and Raman) in comparison to the anions in solution. It was shown that in comparison to free  $\text{CO}_3^{2-}$  a shift towards lower wavenumbers was observed. A band around  $3000\text{--}3200\text{ cm}^{-1}$  has been attributed to the bridging mode  $\text{H}_2\text{O--CO}_3^{2-}$ . The IR spectrum of the  $\text{CO}_3$ -hydrotalcite clearly shows the split  $\nu_3$  around  $1365$  and  $1400\text{ cm}^{-1}$  together with weak  $\nu_2$  and  $\nu_4$  modes around  $870$  and  $667\text{ cm}^{-1}$ . The  $\nu_1$  is activated and observed as a weak band around  $1012\text{ cm}^{-1}$ . The Raman spectrum shows a strong  $\nu_1$  at  $1053\text{ cm}^{-1}$  plus weak  $\nu_3$  and  $\nu_4$  modes around  $1403$  and  $695\text{ cm}^{-1}$ . The symmetry of the carbonate anions is lowered from  $D_{3h}$  to  $C_{2v}$  resulting in activation of the IR inactive  $\nu_1$  mode around  $1050\text{--}1060\text{ cm}^{-1}$ . In addition, the  $\nu_3$  shows a splitting of  $30\text{--}60\text{ cm}^{-1}$ . Although the  $\text{NO}_3$ -hydrotalcite has incorporated some  $\text{CO}_3^{2-}$  the IR shows a strong  $\nu_3$  at  $1360\text{ cm}^{-1}$  with a weak band at  $827\text{ cm}^{-1}$ ,  $\nu_4$  is observed at  $667\text{ cm}^{-1}$ , although it is largely obscured by the hydrotalcite lattice modes. The Raman spectrum shows a strong  $\nu_1$  at  $1044\text{ cm}^{-1}$  with a weaker  $\nu_4$  at  $712\text{ cm}^{-1}$ . The  $\nu_3$  at  $1355\text{ cm}^{-1}$  is obscured by a broad band due to the presence of  $\text{CO}_3^{2-}$ . The symmetry of  $\text{NO}_3^-$  did not change when incorporated in the hydrotalcite. The IR spectrum of the  $\text{SO}_4$ -hydrotalcite shows a strong  $\nu_3$  at  $1126$ ,  $\nu_4$  at  $614$  and a weak  $\nu_1$  at  $981\text{ cm}^{-1}$ . The Raman spectrum is characterised by a strong  $\nu_1$  at  $982\text{ cm}^{-1}$  plus medium  $\nu_2$  and  $\nu_4$  at  $453$  and  $611\text{ cm}^{-1}$ ,  $\nu_3$  can not be identified as a separate band, although a broad band can be seen around  $1134\text{ cm}^{-1}$ . The site symmetry of  $\text{SO}_4^{2-}$  is lowered from  $T_d$  to  $C_{2v}$ . The distortion of  $\text{ClO}_4^-$  in the interlayer of hydrotalcite is reflected in the IR spectrum with both  $\nu_3$  and  $\nu_4$  split around  $1096 + 1145\text{ cm}^{-1}$  and  $626 + 635\text{ cm}^{-1}$ , respectively. A weak  $\nu_1$  is observed at  $935\text{ cm}^{-1}$ . The Raman spectrum shows a strong  $\nu_1$  around  $936\text{ cm}^{-1}$  plus  $\nu_2$  and  $\nu_4$  at  $461$  and  $626\text{ cm}^{-1}$ , respectively.  $\nu_3$  cannot be clearly recognised, but a broad band is visible around  $1110\text{ cm}^{-1}$ . These data indicative a symmetry lowering from  $T_d$  to  $C_s$ .

In this paper we describe the thermal behaviour of these hydrotalcites containing  $\text{CO}_3^{2-}$ ,  $\text{NO}_3^-$ ,  $\text{SO}_4^{2-}$  and  $\text{ClO}_4^-$ . In addition to the weight losses as function of temperature as measured with conventional thermogravimetric analysis and differential thermal analysis, the evolved gasses were analysed by mass spectrometry. This way it is possible to get a better understanding of the mechanisms involved in the decomposition of hydrotalcites containing various anions.

## 2. EXPERIMENTAL METHODS

### 2.1 Synthesis of the Mg/Al-hydrotalcites containing $\text{CO}_3^{2-}$ , $\text{NO}_3^-$ , $\text{Cl}^-$ , $\text{SO}_4^{2-}$ and $\text{ClO}_4^-$

The hydrotalcite with theoretical composition of  $\text{Mg}_6\text{Al}_2(\text{OH})_{16}\text{CO}_3 \cdot n\text{H}_2\text{O}$  was synthesised according to the method described before by Klopogge and Frost (1999). This method comprises the slow simultaneous addition of a mixed aluminium nitrate (0.25M)-magnesium nitrate (0.75M) and a mixed NaOH (2.00M)- $\text{Na}_2\text{CO}_3$  (0.125M) solution under vigorous stirring buffering the pH at approximately 10. The product was washed to eliminate excess salt and dried at 60°C.

The incorporation of carbonate during the synthesis of the hydrotalcites containing the other anions was as much as possible prevented by boiling the deionised water before use, by rinsing the NaOH pellets before use and by executing the synthesis under a nitrogen atmosphere. As sources for the sulphate and perchlorate anions in solution the corresponding magnesium and aluminium salts were used instead of the magnesium and aluminium nitrates as discussed above.

The crystalline nature of the resulting materials was checked by X-ray powder diffraction (XRD). The XRD analyses were carried out on a Philips wide angle PW 1050/25 vertical goniometer equipped with a graphite diffracted beam monochromator. The radiation applied was  $\text{CoK}\alpha$  (1.7902 Å) from a long fine focus Co tube operating at 35 kV and 40 mA. The samples were measured at 50 % relative humidity in stepscan mode with steps of  $0.02^\circ 2\theta$  and a counting time of 2s.

### 2.2. Analytical techniques

Thermoanalytical investigations were carried out in a Netzsch (Selb, Germany) TG 209 type thermobalance in a flowing argon atmosphere of 99.995% purity (Messer Griesheim, Hungary) at a heating rate of 10°C/min. To simultaneously follow the evolution of the gaseous decomposition products over the temperature range investigated, the thermobalance was connected to a Balzers MSC 200 Thermo-Cube type mass spectrometer (Balzers AG, Lichtenstein). The transfer line to introduce gaseous decomposition products into the mass spectrometer was a deactivated fused silica capillary (Infochroma AG, Zug, Switzerland; 0.23 mm o.d.) temperature controlled to 150°C to avoid possible condensation of the evolved gases. In this way the thermogravimetric (TG), derivative thermogravimetric (DTG) and mass spectrometric ion intensity curves of the selected ionic species could be recorded simultaneously.

The finely powdered samples were combined with oven dried spectroscopic grade KBr (containing approximately 1 wt% sample) and pressed into a disc under vacuum. The spectra were recorded in triplicate by accumulating 512 scans at  $4\text{ cm}^{-1}$  resolution in the spectral range between  $400\text{ cm}^{-1}$  and  $4000\text{ cm}^{-1}$  using the Perkin-Elmer 1600 series Fourier transform infrared spectrometer equipped with a LITA detector and on a Nicolet Magna 750 Fourier transform infrared spectrometer equipped with a DTGS detector. The Fourier transform Raman spectroscopic (FT-Raman) analyses were performed on a Perkin Elmer System 2000 Fourier transform spectrometer equipped with a Raman accessory comprising a Spectron Laser Systems SL301 Nd:YAG laser operating a wavelength of 1064 nm. 1000 scans were obtained at a spectral resolution of  $4\text{ cm}^{-1}$  in order to obtain an acceptable signal/noise ratio.

### 3. RESULTS AND DISCUSSION

#### 3.1. Characterisation of the solid materials

All the samples synthesised for this study were identified as Mg/Al-hydrotalcites. Fig. 1 shows the XRD patterns of the synthesised hydrotalcites. The hydrotalcites synthesised with carbonate, nitrate or sulphate as the interlayer anion clearly show one crystalline phase. The value of 7.8 Å is characteristic of the 003 reflection of carbonate containing hydrotalcite (Fig. 1) Replacement of carbonated by nitrate as the interlayer anion results in a slight expansion from 7.8 Å to around 8.1 Å, which is slightly smaller compared to the value of 8.36 Å reported by Marino and Masculo (1982). Incorporation of sulphate gives a 003 reflection of 8.9 Å that agrees well with data reported by e.g. Miyata and Okada (1977), Bish (1980) and Sato et al. (1986). The sample with the perchlorate as the interlayer anion however clearly shows a second phase with a 003 reflection similar to that of a carbonate containing hydrotalcite in addition to a stronger reflection at 9.3 Å, which agrees with data reported by Miyata and Kumura (1973) and Brindley and Kikkawa (1980). A similar observation of two separate phases containing perchlorate and carbonate was made by Brindley and Kikkawa (1979).

Infrared spectroscopy (Fig. 2) was used at this stage to identify the interlayer anions in the hydrotalcites synthesised. This confirmed clearly the presence of carbonate in the perchlorate system. So, even though greatest care was taken to exclude carbonate from the system, carbonate is sometimes found in the interlayer space. A similar observation was made in the infrared spectra of the nitrate containing hydrotalcite, which probably also explains the slightly smaller 003 value and the broadening of the reflection compared to that of the carbonate containing hydrotalcite. Opposite to these observations, the use of nitrate salts in the case of the carbonate containing hydrotalcite resulted in the incorporation of a minor amount of nitrate as well, as was earlier observed by Klopogge and coworkers. (Hickey et al. 2000, Klopogge et al. 2000).

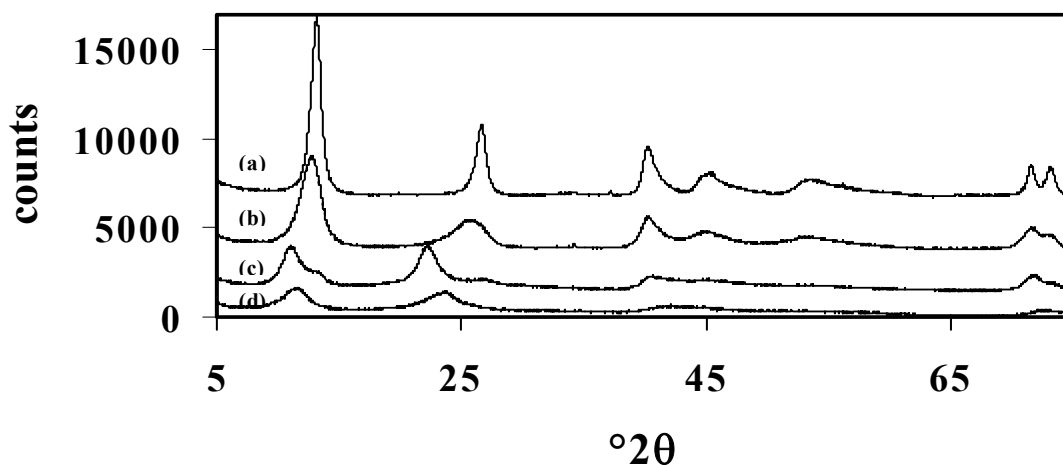


**Fig. 1** XRD patterns of the hydrotalcites containing (a) CO<sub>3</sub><sup>2-</sup>, (b) NO<sub>3</sub><sup>-</sup>, (c) ClO<sub>4</sub><sup>2-</sup> and (d) SO<sub>4</sub><sup>2-</sup>.

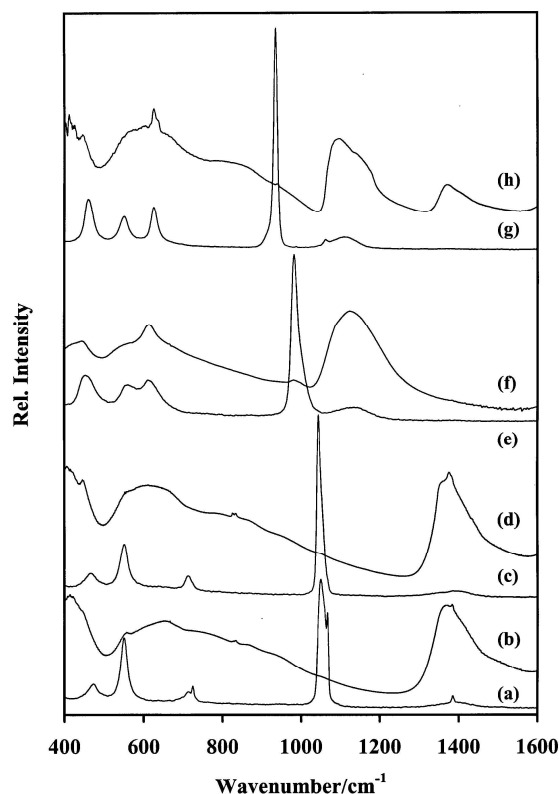


**Fig. 2** Spectra of hydrotalcite containing CO<sub>3</sub><sup>2-</sup> (a) Raman, (b) IR; NO<sub>3</sub><sup>-</sup> (c) Raman, (d) IR; SO<sub>4</sub><sup>2-</sup> (e) Raman, (f) IR and ClO<sub>4</sub><sup>-</sup> (g) Raman and (h) IR.

### 3.2. Thermal behaviour of the anions in hydrotalcite

All the TGA patterns of the hydrotalcites, containing various anions, are characterized by a weight loss between 10 and 20 wt% due to loss of interlayer water with a maximum around 75-115°C. For CO<sub>3</sub>-hydrotalcite (Fig. 3) The dehydration takes place in two minor steps followed by a larger step around 197°C. These steps can be interpreted as being due to the loss of adsorbed water followed by loosely bound interlayer water and finally water coordinated to the interlayer carbonate.

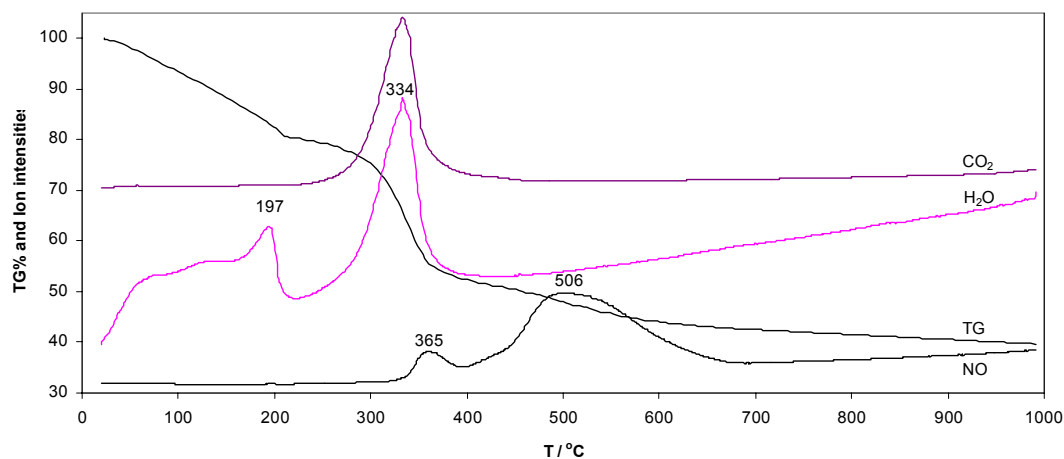


**Fig. 3.** TGA-MS patterns of CO<sub>3</sub>-hydrotalcite.

The three steps of dehydration are also observed in the corresponding differential thermal analysis pattern. The interlayer carbonate is released as  $\text{CO}_2$  simultaneously with water around  $335^\circ\text{C}$  followed by  $\text{NO}$  around  $365$  and  $500^\circ\text{C}$ . This water loss around  $335^\circ\text{C}$  is due to the dehydroxylation of the  $\text{Mg}/\text{Al}$ -hydroxide sheets.

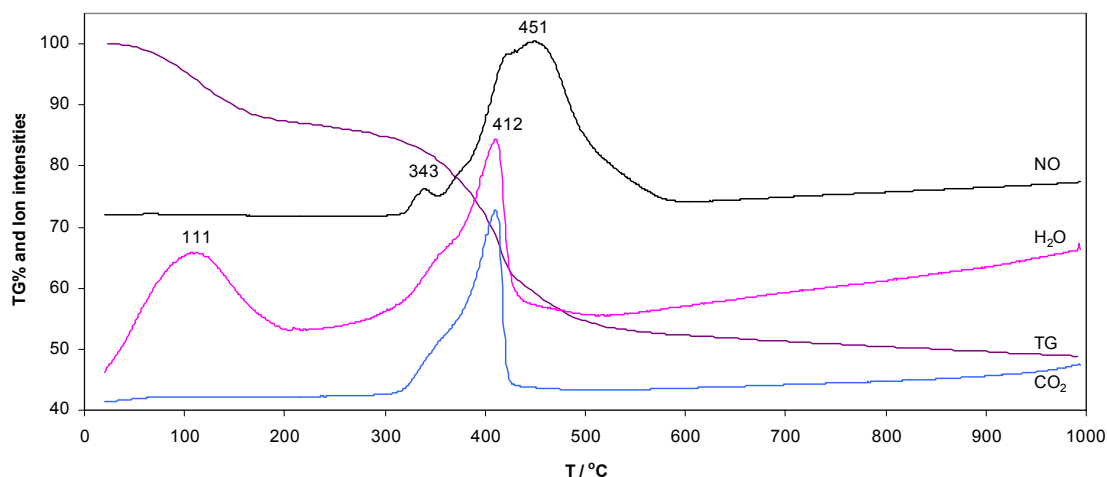


**Fig. 4.** TGA-MS pattern of  $\text{NO}_3$ -hydrotalcite.

The stability of the  $\text{NO}_3$ -hydrotalcite (Fig. 4) is higher than that of the  $\text{CO}_3$ -hydrotalcite (Fig. 3). Since some carbonate was taken up in the hydrotalcite structure during the synthesis as shown by the infrared spectrum a major loss of  $\text{CO}_2$  is observed around  $412^\circ\text{C}$ . The dehydration in this case takes place as a single event over a large temperature range up to  $200^\circ\text{C}$ , while dehydroxylation and the associated loss of  $\text{H}_2\text{O}$  around  $412^\circ\text{C}$ . The interlayer nitrated decomposes to  $\text{NO}$  with a minor loss around  $345^\circ\text{C}$  followed by a major loss around  $450^\circ\text{C}$ . It seems that the presence of nitrate in the interlayer stabilizes the interlayer carbonate resulting in an increase in temperature of about  $80^\circ\text{C}$  before this carbonate is lost. So far, there is no clear explanation for the minor  $\text{NO}$  loss around  $345^\circ\text{C}$ . The presence of  $\text{NaNO}_3$  as a cause can be excluded since  $\text{NaNO}_3$  melts at a higher temperature and decomposition does not take place until  $650^\circ\text{C}$ .

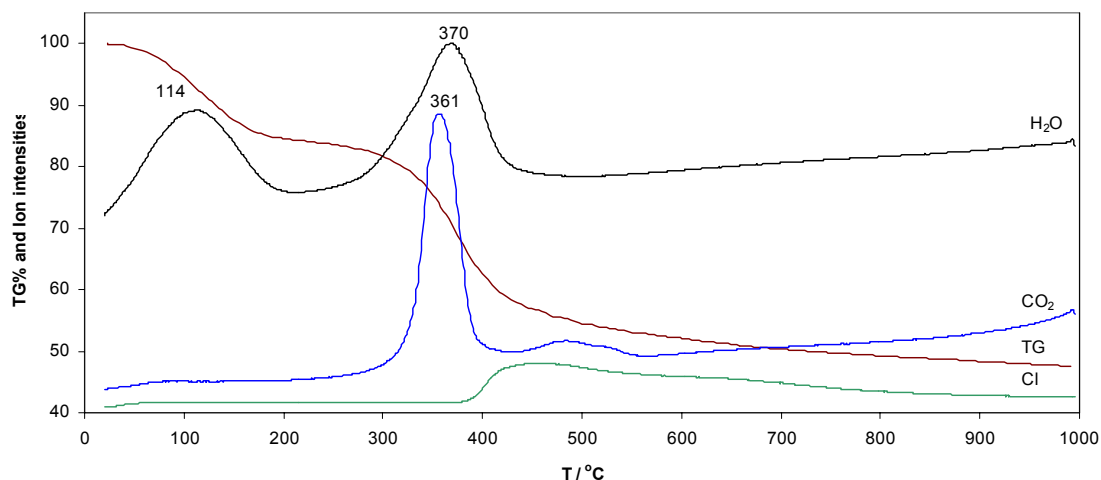


**Fig. 5.** TGA-MS patterns of  $\text{Cl}$ -hydrotalcite.

The Cl-hydrotalcite (Fig. 5) shows a similar behaviour for the H<sub>2</sub>O loss (dehydration) as the NO<sub>3</sub>-hydrotalcite, but Cl is lost over a larger and higher temperature range from 400 to 900°C. As with the nitrate the interlayer chloride anions seems to stabilize the interlayer carbonate as shown by the fact that after the major CO<sub>2</sub> loss around 360°C a second step is observed around 500°C coinciding with the major release of Cl<sub>2</sub>. No HCl was detected.

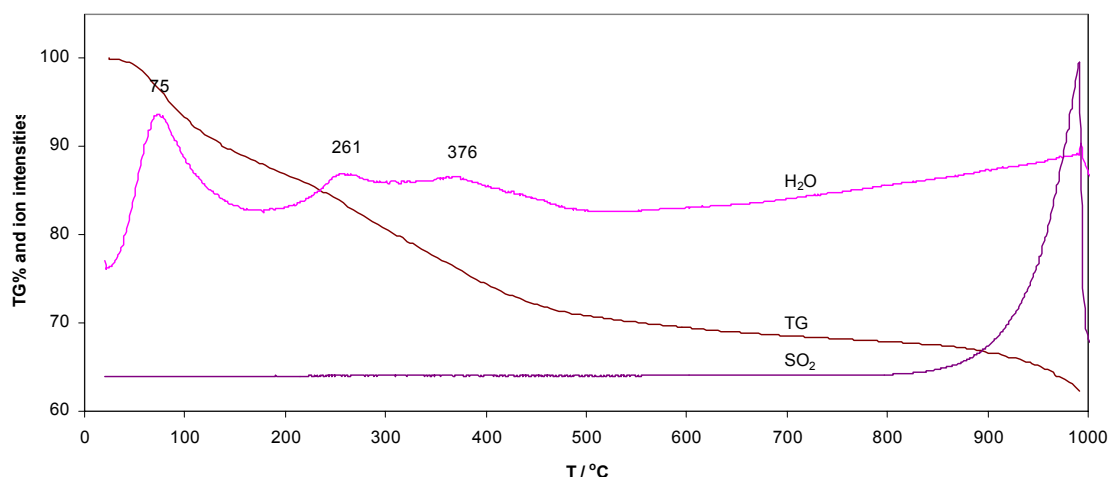


**Fig. 6.** TGA-MS pattern of SO<sub>4</sub>-hydrotalcite.

Completely different is the thermal behaviour of SO<sub>4</sub>- (Fig. 6) and ClO<sub>4</sub>-hydrotalcites (Fig. 7). SO<sub>4</sub>-hydrotalcite shows a gradual weight-loss due to dehydroxylation with two minor water peaks around 260 and 375°C, while the sulphate remains in the structure. The sulphate is not lost as SO<sub>2</sub> until a temperature of 850°C is reached. This may be interpreted as being due to the formation of separate phases of magnesium and aluminium sulphate upon dehydroxylation. The ClO<sub>4</sub>-hydrotalcite shows a complex thermal behaviour with 2 steps of water loss around 375 and 440°C, where the second step is accompanied by the loss of O<sub>2</sub>.

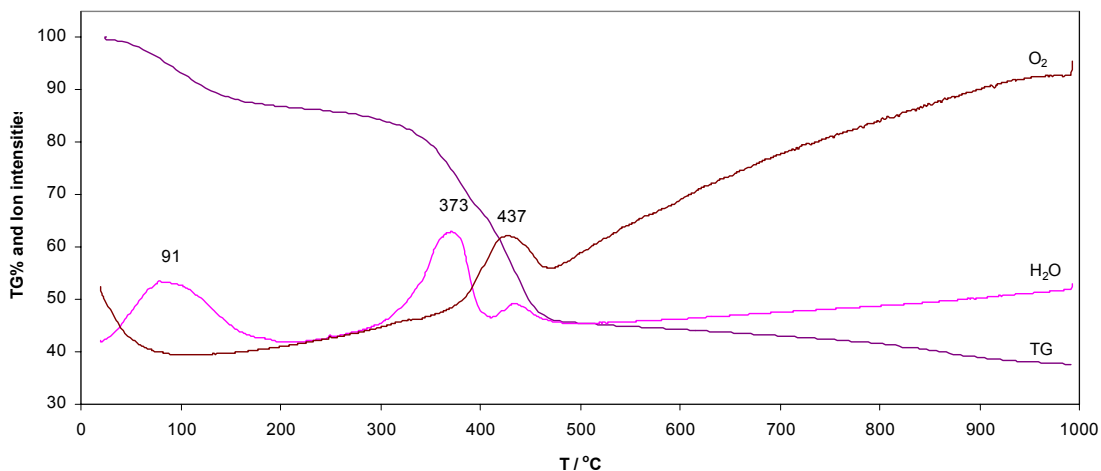


**Fig. 7.** TGA-MS pattern of ClO<sub>4</sub>-hydrotalcite.

## REFERENCES

- Bish, D.L. (1980) Anion-exchange in takovite: applications to other hydroxide minerals. *Bulletin de Mineralogie*, 103, 170-175.
- Brindley, G.W. and Kikkawa, S. (1979) A crystal-chemical study of Mg,Al and Ni,Al hydroxy-perchlorates and hydroxy-carbonates. *American Mineralogist*, 64, 836.
- Brindley, G.W. and Kikkawa, S. (1980) Thermal behavior of hydrotalcite and of anion exchanged forms of hydrotalcite. *Clays and Clay Minerals*, 28, 87-91.
- Hickey, L., Kloprogge, J.T. and Frost, R.L. (2000) The effects of various hydrothermal treatments on Mg/Al - hydrotalcites. *Journal of Materials Science*, 35, 4347-4355.
- Kloprogge, J.T. and Frost, R.L. (1999) Fourier Transform Infrared and Raman spectroscopic study of the local structure of Mg, Ni and Co - hydrotalcites. *Journal of Solid State Chemistry*, 146, 506-515.
- Kloprogge, J.T., Wharton, D. and Frost, R.L. (2000) Raman and infrared spectroscopy of interlayer  $\text{CO}_3^{2-}$ ,  $\text{NO}_3^-$ ,  $\text{SO}_4^{2-}$  and  $\text{ClO}_4^-$  in hydrotalcites. *ICORS 2000*, p. 96, Beijing, China.
- Kloprogge, J.T., Wharton, D., Hickey, L. and Frost, R.L. (2002) Infrared and Raman study of interlayer anions  $\text{CO}_3^{2-}$ ,  $\text{NO}_3^-$ ,  $\text{SO}_4^{2-}$  and  $\text{ClO}_4^-$  in Mg/Al-hydrotalcite. *American Mineralogist*, 87, 623-629.
- Marino, O. and Mascolo, G. (1982) Thermal stability of MgAl double hydroxides modified by anionic exchange. *Thermochimica Acta*, 55, 377-383.
- Miyata, S. and Kumura, T. (1973) Synthesis of new hydrotalcite-like compounds and their physico-chemical properties. *Chemistry Letters*, 843-848.
- Miyata, S. and Okada, A. (1977) Synthesis of hydrotalcite-like compounds and their physico-chemical properties - the system  $\text{Mg}^{2+}$  -  $\text{Al}^{3+}$  -  $\text{SO}_4^{2-}$  and  $\text{Mg}^{2+}$  -  $\text{Al}^{3+}$  -  $\text{CrO}_4^{2-}$ . *Clays and Clay Minerals*, 25, 14-18.
- Sato, T., Wakabayashi, T. and Shimada, M. (1986) Adsorption of various anions by magnesium aluminium oxide ( $\text{Mg}_{0.7}\text{Al}_{0.3}\text{O}_{1.15}$ ). *Industrial & Engineering Chemistry Product Research and Development*, 25, 89-92.
- Titulaer, M.K. (1993) Porous Structure and Particle Size of Silica and Hydrotalcite Catalyst Precursors, *Geologica Ultraiectina* 99, p. 268. Utrecht University, Utrecht, The Netherlands.
- Vaccari, A. (1998) Preparation and Catalytic properties of cationic and anionic clays. *Catalysis Today*, 41, 53-71.